SO_2 ABSORPTION BY WATER DROPLETS

RYUICHI KAJI AND YUKIO HISHINUMA
Hitachi Research Laboratory, Hitachi 319-12
HIROSHI KURODA
Babcock-Hitachi K.K., Kure 737

Key Words: Desulfurization, Absorption, Spray Scrubber

Introduction

Removal of SO_2 from gases by absorption is an important process for air pollution control. A knowledge of gas- and liquid-film mass transfer coefficients for absorption of SO_2 by water droplets is of importance in designing spray scrubbers for this purpose. Although extensive studies have been made on the gas-film mass transfer coefficient around a sphere since the work of Frössling,[3] the mass transfer coefficient within a liquid droplet has not been fully investigated.

In this paper, the authors report experimental results on the liquid-film mass transfer coefficient for the absorption of SO_2 by water droplets.

1. Experimental

Experiments were carried out using the apparatus illustrated in **Fig. 1**. A mixture of SO_2 and nitrogen with SO_2 concentration of 620, 1126, or 1968 ppm was passed through the absorption column (41 mm i.d.). The gas was saturated with water vapor, before it was fed to the column, by passing the nitrogen gas through a humidifier. The linear velocity of the gas in the column was kept at 3.3 $cm \cdot s^{-1}$ at 20°C by regulating its volumetric flow rate with calibrated rotameters.

Distilled water and NaOH solution of 0.01 $mol \cdot dm^{-3}$ were used as absorbents. Ten cm^3 of the absorbing liquid was fed by a precision syringe feeder to a hypodermic needle by which droplets of a constant diameter of 2.2 mm were formed, approximately every 2 seconds. The droplet diameter was determined separately by collecting thirty droplets and weighing them. The surface area of the droplets was calculated on the assumption that they were spheres. The droplet formation section was purged with a small amount of nitrogen to prevent absorption of SO_2 during drop formation.

The droplets were collected in a cup placed at the bottom of the absorption column for analysis. Concentrations of the absorbed SO_2 were determined by iodometry. A kerosene film was used to shield the collected liquid from the gas stream. Preliminary experiments showed that it was effective for this purpose. The length of the absorption column was varied from 23 to 113 cm, which corresponds to contact times of 0.155 to 0.431 second. All experiments were carried out in a room where the temperature was kept at 20 ± 1°C.

2. Absorption Rate

The fundamentals of the process involved in the absorption of sulfur dioxide in water are shown by the following reactions[2]

$$SO_2(g) + H_2O \rightleftharpoons SO_2(l) + H_2O \rightleftharpoons HSO_3^- + H^+ \quad (1)$$

$$HSO_3^- \rightleftharpoons SO_3^- + H^+ \quad (2)$$

The first part of reaction (1) represents the equilibrium at the gas-liquid interface. Henry's law was shown to describe the equilibrium between $SO_2(g)$ and $SO_2(l)$.[8]

$$H \cdot P^i_{SO_2} = A^i \quad (3)$$

The second part of reaction (1) corresponds to the hydrolysis of absorbed SO_2. The forward rate constant for the reaction at 20°C has been measured as $3.4 \times 10^6\ s^{-1}$ by Eigen *et al.*[1] and the reaction can be

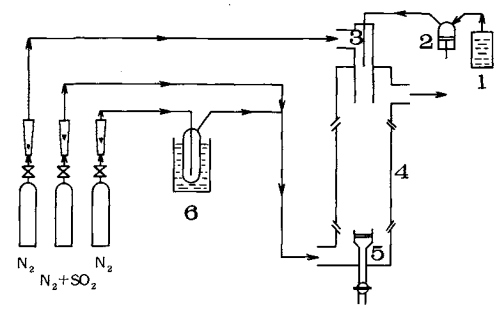

Fig. 1. Schematic diagram of experimental apparatus. 1, water reservoir; 2, feeder; 3, hypodermic needle; 4, absorption column; 5, receiving cup; 6, humidifier.

Received May 15, 1984. Correspondence concerning this article should be addressed to R. Kaji.

regarded as instantaneous.

The second ionization reaction (2) is so small in the aqueous solution of SO_2 that it may be safely neglected.[7] Hence, the absorption of SO_2 into water may be regarded as a mass transfer process accompanied by an instantaneous reaction of the form $A \rightleftarrows E+F$. For this case, the absorption rate is given by[5]

$$N_A = k_L\beta(A^i - A^o) = k_G(P^o_{SO_2} - P^i_{SO_2}) \tag{4}$$

with

$$\beta = 1 + \frac{D^*_{HSO_3^-}}{D_{SO_2(1)}} \frac{\sqrt{K}}{\sqrt{A^i} + \sqrt{A^o}} \tag{5}$$

Rearranging Eq. (4) yields

$$N_A = \left(\frac{1}{k_G} + \frac{1}{k_L\beta H}\right)^{-1} \left(P^o_{SO_2} - \frac{A^o}{H}\right) \tag{6}$$

3. Data Analysis

The average concentration of total dissolved SO_2 in the droplet is expressed by

$$c_t = \frac{1}{V_p} \iint N_A \, da \, dt \tag{7}$$

By assuming that k_G and $k_L \cdot \beta$ are constant at all points of the interface, integration over the surface area can be carried out. The time derivative of c_t then becomes

$$\frac{dc_t}{dt} = \frac{a}{V_p} N_A \tag{8}$$

Combining Eqs. (6) and (8) and rearranging yields

$$K_L = \left(\frac{a}{V_p} \frac{P^o_{SO_2} - A^o/H}{dc_t/dt} - \frac{1}{k_G}\right)^{-1} \frac{1}{\beta \cdot H} \tag{9}$$

To obtain dc_t/dt, the data points were fitted to a hyperbolic curve

$$z = a_1 c_t + a_2 c_t^2 \tag{10}$$

where a_1 and a_2 were determined by the method of least squares. Then

$$\frac{dc_t}{dt} = \frac{dc_t}{dz}\frac{dz}{dt} = \frac{dc_t}{dz} V \tag{11}$$

And from Eq. (10)

$$\frac{dc_t}{dz} = \frac{1}{2a_2}\left\{\frac{z}{a_2} + \left(\frac{a_1}{2a_2}\right)^2\right\}^{-1/2} \tag{12}$$

The A^i involved in β was calculated by the following equation, obtained from Eqs. (3), (4), (8), and (11).

$$A^i = H\left(P^o_{SO_2} - \frac{V_p}{ak_G}\frac{dc_t}{dz} V\right) \tag{13}$$

The gas-film mass transfer coefficient was calculated by the equation proposed by Frössling[3]

Table 1. Physical properties

ρ_G	$=0.001165$	$g \cdot cm^{-3}$
ρ_L	$=0.998$	$g \cdot cm^{-3}$
μ_G	$=0.0001766$	$g \cdot cm^{-1} \cdot s^{-1}$
D_G	$=0.122$	$cm^2 \cdot s^{-1}$
$D_{HSO_3^-}$	$=1.29 \times 10^{-5}$	$cm^2 \cdot s^{-1}$
D_{H^+}	$=8.13 \times 10^{-5}$	$cm^2 \cdot s^{-1}$
$D_{SO_2(1)}$	$=1.40 \times 10^{-5}$	$cm^2 \cdot s^{-1}$
H	$=1.39 \times 10^{-5}$	$mol \cdot dm^{-3} \cdot Pa^{-1}$
K	$=0.0145$	$mol \cdot dm^{-3}$

$$Sh = 2(1 + 0.276 Re^{1/2} Sc^{1/3}) \tag{14}$$

The Henry constant and the dissociation constant for reaction (1) were calculated from the equation suggested by Rabe and Harris.[8] The diffusion coefficient of SO_2 in the gas phase was calculated by way of the Chapman-Enskog formula.[6] The diffusion coefficients of H^+, HSO_3^-, and $SO_2(1)$ at 20°C were calculated from the values given in Roberts and Friedlander[9] using the correlation $D \cdot \mu_L/T = \text{const.}$ The values are summarized in **Table 1** together with other physical properties used in the calculation. The effective diffusivity of HSO_3^- was obtained from

$$D^*_{HSO_3^-} = \frac{2D_{HSO_3^-} D_{H^+}}{D_{HSO_3^-} + D_{H^+}} \tag{15}$$

The falling velocity of the droplet, V, in the absorption column was calculated by numerically integrating the equation of motion using the drag coefficient

$$c_D = \frac{10}{\sqrt{Re}} \tag{16}$$

The calculated velocities agreed very well with the velocities measured by photographic means using a stroboscope.

4. Results and Discussion

Since the accuracy of the liquid-film mass transfer coefficients obtained in this study is dependent on the accuracy of the gas-film mass transfer coefficient calculated from Eq. (14), the applicability of Eq. (14) to the present system was checked by performing experiments using 0.01 $mol \cdot dm^{-3}$ NaOH solution as an absorbent. The results are shown in **Fig. 2**. The solid line in the figure indicates the calculated value for the case of $k_L = \infty$, where the resistance to mass transfer is solely in the gas phase. The experimental results are in excellent agreement with the calculated values, proving the applicability of Eq. (14) to this study. This result is also considered to indicate that the end effects may have been negligible.

The average concentrations of total SO_2 absorbed by water droplets, c_t, are plotted in **Fig. 3**. The solid lines in the figure are simulated curves obtained from

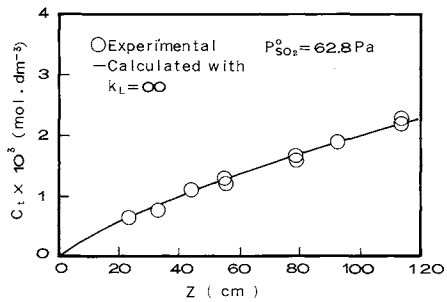

Fig. 2. Results of SO_2 absorption by droplets of 0.01 mol·dm^{-3} NaOH solution.

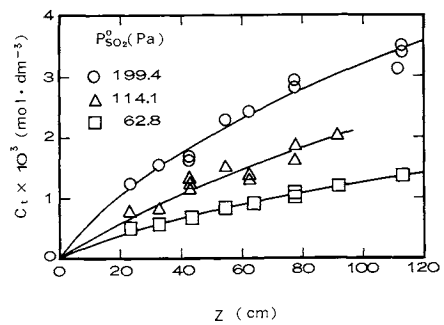

Fig. 3. Results of SO_2 absorption by water droplets.

Eq. (10).

The liquid-film mass transfer coefficients and the enhancement factors obtained from the simulated curves by way of Eqs. (9), and (5) and (13) are plotted in **Fig. 4**. The liquid-film mass transfer coefficients are independent of the SO_2 concentration in the gas phase and have a value between 55 and 70 kmol·m^{-2}·h^{-1}. The enhancement factor decreases with SO_2 concentration in the gas phase due to the increase in SO_2 concentration at the gas-liquid interface.

Mass transfer to a liquid sphere with internal circulation has been studied theoretically by Handlos and Baron.[4] They gave an equation for liquid-film mass transfer coefficient under the assumption that the transfer process is by eddy diffusion and that the internal flow field is expressed by Hadamard's equation. The dotted line in Fig. 4 shows the calculated value using their equation. The discrepancy at shorter contact times may be due to internal circulation created by liquid flow through the hypodermic needle during the formation period, which might be stronger than that caused by the frictional forces from the gas phase. But the theoretical value for k_L increases with contact time due to the increase in velocity of the droplet. The experimental values decrease with contact time due in part to the decrease in initial internal circulation. It seems that the experimental values would become smaller than the theoretical ones at contact times longer than 0.4 s. This may suggest that A^0 may not maintain its initial value because of the mixing within the droplet caused by internal circulation.

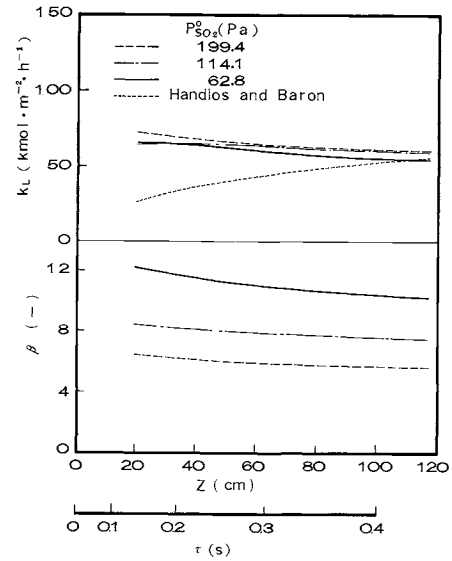

Fig. 4. Liquid film mass transfer coefficients and enhancement factors for SO_2 absorption by water droplets.

Nomenclature

a	=	surface area of a droplet	[cm^2]
A	=	concentration of SO_2 in water	[mol·dm^{-3}]
c_t	=	total concentration of SO_2 in liquid phase	[mol·dm^{-3}]
c_D	=	drag coefficient	[—]
d	=	diameter of a droplet	[cm]
D	=	diffusivity in water	[cm^2·s^{-1}]
$D^*_{HSO_3^-}$	=	effective diffusivity of HSO_3^-	[cm^2·s^{-1}]
D_G	=	molecular diffusivity of SO_2 in gas phase	[cm^2·s^{-1}]
H	=	Henry constant	[mol·dm^{-3}·Pa^{-1}]
k_G	=	gas-film mass transfer coefficient	[mol·cm^{-2}·s^{-1}·Pa^{-1}]
k_L	=	liquid-film mass transfer coefficient	[kmol·m^{-2}·h^{-1} or cm·s^{-1}]
K	=	dissociation constant for Eq. (1)	[mol·dm^{-3}]
N_A	=	absorption rate	[mol·cm^{-2}·s^{-1}]
P	=	total pressure of gas phase	[Pa]
P_{SO_2}	=	partial pressure of SO_2	[Pa]
Re	=	$\dfrac{\rho_G \cdot U \cdot d}{\mu_G}$	[—]
Sc	=	$\dfrac{\mu_G}{\rho_G \cdot D_G}$	[—]
Sh	=	$\dfrac{k_G \cdot R \cdot T \cdot d}{D_G P}$	[—]
t	=	time	[s]
T	=	absolute temperature	[K]
U	=	relative velocity of a droplet	[cm·s^{-1}]
V	=	velocity of a droplet	[cm·s^{-1}]
V_p	=	volume of a droplet	[cm^3]
z	=	distance along absorption column	[cm]
β	=	enhancement factor	[—]
μ	=	viscosity	[g·cm^{-1}·s^{-1}]
ρ	=	density	[g·cm^{-3}]
τ	=	contact time	[s]

〈Subscripts〉

G	=	gas phase
L	=	liquid phase

〈Superscripts〉

i = at the interface

o = in the bulk

Literature Cited

1) Eigen, M., K. Kustin and G. Maass: *Z. Phys. Chem.*, **30**, 130 (1961).
2) Eriksen, T. E.: *Chem. Eng. Sci.*, **24**, 273 (1969).
3) Frössling, N.: *Beitr. Geophys.*, **52**, 170 (1938).
4) Handlos, A. E. and T. Baron: *AIChE J.*, **3**, 127 (1959).
5) Hikita, H., S. Asai and H. Nose: *AIChE J.*, **24**, 147 (1978).
6) Hirschfelder, J. O., C. F. Curtiss and R. B. Bird: "Molecular Theory of Gases and Liquids," Wiley, New York (1954).
7) Morgan, O. M. and O. Maass: *Can. J. Res.*, **5**, 162 (1931).
8) Rabe, A. E. and J. F. Harris: *J. Chem. Eng. Data*, **8**, 333 (1963).
9) Roberts, D. L. and S. K. Friedlander: *AIChE J.*, **26**, 593 (1980).

GAS HOLDUP IN DOWNFLOW BUBBLE COLUMNS WITH GAS ENTRAINMENT BY A LIQUID JET

AKIRA OHKAWA, YOSHIHIRO SHIOKAWA AND NOBUYUKI SAKAI

Department of Chemical Engineering, Niigata University, Niigata 950-21

KAZUO ENDOH

Department of Chemical Process Engineering, Hokkaido University, Sapporo 060

Key Words: Dowlflow Bubble Column, Liquid Jet, Gas Entrainment, Gas Holdup, Chemical Reactor

Downflow bubble columns, in which the gas is dispersed at the top of the column in a liquid flowing cocurrently and thereby the bubbles are forced downward in a direction opposite to their buoyancy, have become of interest lately.[2-6,12,13] This system has the advantage that the gas residence time can be considerably increased as compared with that in the bubble column where the gas is dispersed from the bottom. The downflow system of present concern is identical to the above downflow bubble column in gas-liquid contacting mechanism but different in the method of supplying the gas. The objective of this study is to investigate the changes in gas holdup in downflow bubble columns with gas entrainment, and to compare the results with those in bubble columns with gas sparging.

1. Experimental

A schematic diagram of the experimental setup is shown in **Fig. 1**. The apparatus comprised four parts: liquid feed nozzle, column, separation tank and liquid circulation pump. The main body of the apparatus was made of transparent acrylic resin. In operation, liquid was first introduced downward through the short cylindrical nozzle (made of PVC) at the top of the column. The gas entrained by this liquid jet then produced gas bubbles in the liquid in the column. The mixed-phase flow of gas-liquid formed was forced out from the lower end of the column in a separation tank (0.14 m in diameter and 0.27 m in height) by the downward flow developed. The liquid separated from the gas in the separation tank was circulated back to the column by a pump. In experiments, the aerated liquid height H_f from the lower end of the column was held constant at 2.0 m, but the diameters of the column and nozzle or the liquid jet length were varied within the range shown in **Table 1**.

In measuring the volume of gas entrained through the column, the gas separated in the tank was introduced into a replacement vessel. By measuring the volume of liquid replaced by the gas,[7] the volumetric rate of entrained gas was determined. The mean gas holdup based on H_f was measured by two different methods: the overflowing method[8,10] and the method based on the pressure balance in the apparatus. It was ascertained that the values of gas holdup by these two

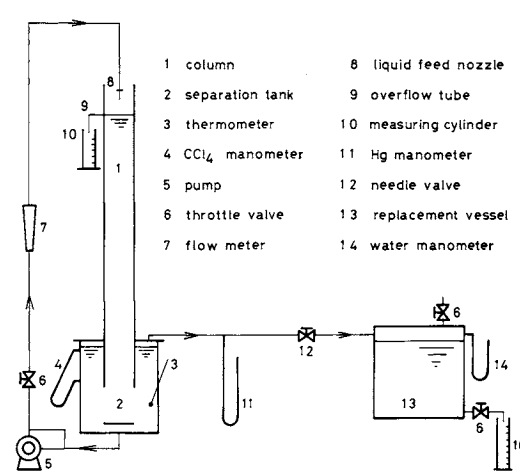

Fig. 1. Schematic diagram of experimental apparatus.

Received June 14, 1984. Correspondence concerning this article should be addressed to A. Ohkawa.